New Journal of Physics
The open–access journal for physics

Orbital ordering in transition-metal spinels

Paolo G Radaelli

ISIS Facility, Rutherford Appleton Laboratory, CCLRC, Chilton, Didcot, Oxon OX11 0QX, UK
Department of Physics and Astronomy, University College London, Gower Street, London WC1E 6BT, UK
E-mail: P.G.Radaelli@rl.ac.uk

New Journal of Physics **7** (2005) 53
Received 22 October 2004
Published 14 February 2005
Online at http://www.njp.org/
doi:10.1088/1367-2630/7/1/053

Abstract. Transition-metal spinels (general formula AB_2X_4) have been, for many years, the subject of intense experimental and theoretical activity. Structurally, the most interesting feature of these systems is the fact that the *B* cation occupies the nodes of a pyrochlore lattice, which is known to be geometrically frustrated. Therefore, one can explore how the natural tendency of the transition metals to order in the charge, magnetic and orbital sectors is affected by geometrical frustration. Recently, orbital ordering has become a topical subject in a variety of both non-frustrated systems, such as manganites and other perovskites, and in the spinels. In this paper, I review the recent experimental activity on the subject of orbital ordering in transition-metal spinels and relate this to models of orbital ordering that are being developed by theoreticians.

PII: S1367-2630(05)88250-3

Contents

1. Introduction

The term 'geometrical frustration' refers to situations where local order, as established by local interactions, cannot be freely propagated throughout space. This general paradigm has been applied to rather different classes of problems. For example, 'geometrical frustration' is used to describe the non-trivial packing of polyhedra in three-dimensional space in systems such as quasi-crystals and amorphous metals. In other cases, the lattice geometry is defined *a priori*, and the configurational space is provided by tensor fields (scalar, axial or polar vector etc) defined on that lattice. Here, frustration can be induced as a result of randomness in the sign of the interactions (the so-called 'spin-glass' frustration), by finely balancing interactions with different ranges, or, in some cases, even in the presence of a homogeneous and isotropic nearest-neighbour interaction [1]. The latter is only possible on particular lattices, generally based on triangular plaquettes, which have become collectively known as geometrically frustrated (or frustrating) lattices, although the type of interaction and the ordering field are also crucial in establishing whether or not the system is frustrated and, if so, whether the ground state is unique or degenerate at the classical and quantum levels.

Ordering on geometrically frustrated lattices is a time-honoured subject of studies, which preceded the above definitions by several decades, and can be traced back to the work of Linus Pauling on proton disorder in ice [2]. Pauling noted that the proton configurations in ordinary hexagonal ice (ice I_h) could be described as displacement fields away from the nodes of the 'β-tridymite lattice', which defines, for example, the oxygen positions in one of the hexagonal high-temperature forms of SiO_2. The geometry of this lattice is such that there are many different ways to accommodate local proton displacements obeying the 'two-in–two-out' Bernal–Fowler rules [3], and this provided the means to calculate the residual entropy of ice at low temperatures. Most of the subsequent solid-state physics research has focused on the closely related 'β-cristobalite lattice' (β-cristobalite is a cubic high-temperature form of SiO_2), better known as the pyrochlore lattice. Pyrochlores, with the general formula $A_2B_2X_7$, have two interpenetrating

cation lattices with the same topology as that of oxygen in β-cristobalite, which are occupied by an alkali, alkaline earth or rare earth metal (A site) and by a transition metal (B site). Proton configurations in cubic ice I_c map onto this lattice, which, in addition to pyrochlores is also shared by another important class of minerals: the spinels. Spinels, with the general fomula AB_2X_4, have only one pyrochlore lattice, generally occupied by a transition metal or by aluminium, although partial substitutions with other cations are possible (see below). Since the very beginning, it was recognized that the peculiar geometrical properties of these lattices give rise to a very large number of ordered and disordered configurations with very similar energy. This observation was the key in Pauling's explanation of the residual low-temperature entropy of ice. However, it was also assumed that ordering on these lattices is possible, under suitable circumstances. In his classic work on Fe_3O_4 (magnetite), dated 1939 [4], Verwey proposed that ordering of electric charges upon the B-site pyrochlore lattice of this 'inverse spinel'[1] was at the origin of a sharp increase of the electrical resistivity upon cooling below $\sim$120 K (the 'Verwey' transition). Anderson [5] was the first to recognize the existence of a mapping between three ordering problems on the pyrochlore lattice: the proton ordering in ice, the Verwey charge ordering and the ordering of Ising spins. The mapping is exact if only nearest-neighbour interactions are considered. By now, many experimental realizations of these and some closely related models are known, including a variety of magnetic systems. Particularly noteworthy is the discovery of the spin ices, some of which realize the Anderson paradigm in the context of a predominantly nearest-neighbour ferromagnetic (FM) interaction of spins, and in the presence of strong on-site anisotropy [6].

Regardless of the specific implementation, geometrical frustration is intimately intertwined with all these phenomena, since, at the classical mean field level, spin or charge configurations minimizing nearest-neighbour Coulomb or exchange energy form a degenerate lowest energy manifold. In most cases, this induces a suppression of the ordering temperatures much below what is expected based on the strength of the interactions. How the degeneracy is eventually lifted on cooling is a matter of intense theoretical and experimental interest, but, essentially, there are three possibilities. The system can retain its cubic symmetry, remains fluctuating down to low temperatures and may eventually settle in an 'exotic' quantum ground state such as a 'spin liquid', with unusual excitation spectra. A second possibility, which is realized in ice, is that the system 'freezes' in a disordered configuration, such as a spin glass, with residual low-temperature entropy. Alternatively, the system can lift the degeneracy, resulting in long-range charge or spin ordering. This is usually accompanied by a distortion of its crystal structure. When the latter happens, the resulting crystal structures are usually extremely complex, and only a handful of cases have been solved to date. Furthermore, the physics underpinning the symmetry lowering is poorly understood. No example enshrines the current uncertainty about both the experimental and theoretical situation better than the case of magnetite. Sixty-five years after it was first proposed, not only is the full charge-ordered structure still unsolved, but also the very concept of charge ordering (CO) in this system is challenged by many. Indeed, the complex pattern of atomic displacements below the Verwey transition [7] and the lack of spectroscopic evidence for CO [8] are not easily reconciled with a purely ionic model of CO. Prompted by these results,

[1] All spinels have the general formula AB_2X_4. There are two types of metal sites in the structure, with tetrahedral and octahedral coordination, the latter being double in number than the former. In normal spinels, such as chromite ($FeCr_2O_4$), the A cation (in this case Fe) occupies the tetrahedral site (known also as the A site) and the B cation (in this case, Cr) occupies the octahedral site. In inverse spinels, such as magnetite ($Fe^{3+}Fe^{2.5+}{}_2O_4$), the tetrahedral site is occupied by B-type cations (Fe^{3+}), while the octahedral site is shared between A and B cations. Many spinels can be synthesized in intermediate situations between normal and inverse.

among others, the CO paradigm is presently undergoing a radical change: the conventional 'ionic' view of distinct integral valences is clearly not applicable to most situations. However, in the presence of covalency, partial CO is a perfectly acceptable concept, characterized by the fact that Brillouin zone folding, associated with a structural distortion, induces a charge density modulation on previously equivalent sites. Further to this, band structure calculations frequently indicate that these changes are partially or totally screened by modulations of opposite phase in the 'inactive' orbitals (below the Fermi level), so that, paradoxically, CO could occur in the absence of significant charge modulation. Many contend that the name 'charge ordering' is no longer justified in this situation, but no alternative has so far emerged, and CO as a concept, with the appropriate caveats, still retains its validity.

The subject of orbital ordering (OO) also has a long tradition in solid-state physics. OO occurs when the orbital degeneracy of an extended concentrated system is lifted, typically through an interaction with the lattice [9]. This is usually but not always accompanied by a reduction in point-group symmetry of the relevant atomic site. Cases where orbital occupancy is 'significantly' (see below) modulated between two previously equivalent sites, so that symmetry operators involving translations are violated, are often described as 'simultaneous charge/orbital ordering' (CO/OO). Many of the previous considerations on the definition of CO also apply to OO. It is worth remarking that, in principle, any decrease in point-group symmetry results in at least partial lifting of the orbital degeneracy, no matter how small the displacements are. Likewise, any splitting of crystallographic sites is bound to entail differences in the total electron charges, and the development of a superstructure will result in band splitting at the new zone boundary. However, these are important rather than parasitic effects only if the resulting change in electronic energy is the dominant factor driving the structural transition. One may strongly suspect that this is so if the structural transition is accompanied by a large change in transport properties, like in a metal–insulator transition, but the case remains to be proven. Ultimately, this can only be accomplished by reliable band structure calculations, whereby the contribution of the different atomic orbitals to the electronic structure is analysed in detail, and this is often beyond current capabilities for all but the simplest systems. However, this does not prevent theoreticians from building simplified models of CO/OO to describe the most relevant phenomenology.

The best-known case of OO is of course the cooperative Jahn–Teller (JT) distortion [10] as observed, for example, in $LaMnO_3$ [11]. In this and other similar cases where a JT-active ion is involved, the electrons have a strong tendency to localize and the on-site distortion of the coordination shell usually occurs at high temperatures, resulting in a gain of on-site electronic/elastic energy. On cooling, the distorted coordination polyhedra 'crystallize' and form a regularly tiled lattice. When significant electronic hopping takes place, the cooperative JT distortion paradigm is no longer sufficient. The main difficulty is that, in the presence of OO, hopping amplitudes become strongly anisotropic, and depend on the occupancy of orbitals and on their orientation on adjacent sites, as well as on the spins of the electrons involved in the hopping. This physics has been encapsulated in the so-called Kugel–Khomskii (KK) model [12]–[14], which has been successfully applied to a variety of systems (see for example [15]). Most of the theoretical and experimental work has so far concentrated on systems containing transition metal ions with partially filled e_g orbitals. These tend to display the strongest JT effects, with direct coupling to the lattice, due to the fact that the orbitals in question directly point towards the ligands, and hybridize (mainly) with s orbitals of the anion. The states near the Fermi surface have anti-bonding character and are very sensitive to cation–anion distances. More recently, significant attention has been devoted to the possibility of orbital ordering in ions

where only t_{2g} orbitals are occupied, such as Ti^{3+} and V^{4+} ($3d^1$) and V^{3+} ($3d^2$). With respect to e_g systems, t_{2g} systems have a greater degeneracy and weaker coupling to the lattice and can also be strongly affected by the spin–orbit interaction. Both theory and experiments have up to now focused mostly on unfrustrated systems, such as the perovskites (e.g. RE TiO_3 [15], RE stands for rare earth or La) and corundum (V_2O_3: see for example [16, 17]) lattices. In a recent paper, Khomski and Mostovoy have discussed the possible interplay between orbital degeneracy and geometrical frustration [9]. Their work focused mostly on e_g systems such as $LiNiO_2$ (containing a triangular Ni lattice), but some of their conclusions could also be applied to t_{2g} systems. In general, it is fair to say that the field of t_{2g} OO on frustrated lattices, and the pyrochlore lattice in particular, is still relatively new. Few systems have been investigated experimentally, and the theoretical framework to understand them is presently being developed.

In this paper, I will review some of the past and current work on OO in the spinels, focusing on systems with partially filled t_{2g} orbitals. I will mostly describe the experimental situation, with a focus on the structural work that, in my view, underpins any further investigation. However, I will also attempt to describe some recent theoretical progress, with particular emphasis on the attempts to understand the complex patterns of atomic displacements within a unified framework.

2. Conditions for orbital ordering

As already mentioned, here I will consider systems that are elementally ordered on both the A and the B sites, whilst allowing for valence disorder on the latter. The allowed oxidation states for the spinel A site are 1+ (e.g., Li^{1+}, Cu^{1+}), 2+ (the most common case, e.g., Mg^{2+}, Zn^{2+}, Cd^{2+}) and 3+ (e.g., Fe^{3+}, Al^{3+}, Ga^{3+}). Spinels with 4+ valence state for the A site are known to exist as high-pressure forms of olivine minerals (e.g. $SiCo_2O_4$, $SiFe_2O_4$). In combination with a 2-anion, these four A-site oxidation states yield formal valences of 3.5+, 3+, 2.5+ and 2+, respectively, for the B site. All chalcogenides except polonium (i.e., O, S, Se and Te) are known to form transition-metal spinels.

The main prerequisite for OO is the presence of a degenerate ground state of the B-site ion. The most important cases are those of 'pure' t_{2g} or e_g systems, in which the 'orbitally active' levels are partially filled, whereas the others are unfilled, half-filled or full. In principle, other electronic configurations ('intermediate spin' states) are possible when the ground state is determined neither by the Hund's rule nor by the crystal field. In practice, however, none of these has been shown to be relevant in spinels. In the case of pure e_g ions, such as Mn^{3+} and Cu^{2+}, the on-site JT energy is usually dominant, with a large distortion of the ligand shell. A trivial case is that of single-valence Mn^{3+}, such as in $ZnMn_2O_4$ [18, 19]: the space group is $I4_1/amd$, with $a_T \sim a_c/\sqrt{2}$ and $c_T \sim a_c$,[2] and a strong tetragonally elongated distortion ($c_T/a_T\sqrt{2} \sim 1.14$) stabilizes $d_{3z^2-r^2}$ occupancy for all octahedra. A much less trivial case is that of the mixed-valence (Mn^{3+}/Mn^{4+}) compound $LiMn_2O_4$ [20]. The structure is orthorhombic but close to being tetragonal, with space group Fddd and $a_0 \sim b_0 \sim 3a_c$ and $c_0 \sim a_c$. The predominant distortion is a pseudo-tetragonal compression, suggesting that the filled orbitals are predominantly lying in the a–b plane. This is confirmed by the analysis of the internal structural parameters, which also reveal a structure of intriguing complexity. There are 144 Mn sites of five distinct types in the unit cell, three with '3+' character (Mn(1), Mn(2) and Mn(3)) and two with '4+' character (Mn(4)

[2] Here, a_c is the cubic lattice parameter, and a_T and c_T the tetragonal lattice parameters.

Table 1. Examples of B site electronic configurations in transition-metal spinels. HS and LS mean high spin and low spin, respectively.

No orbital degeneracy					
$n\mathrm{d}^0$	$n\mathrm{d}^3$	$n\mathrm{d}^5$ HS	$n\mathrm{d}^6$ LS	$n\mathrm{d}^8$	$n\mathrm{d}^{10}$
$CdSc_2S_4$, $LiTi_2O_4$[a]	$ZnCr_2O_4$	$ZnFe_2O_4$	–	$SiNi_2O_4$[b]	–
t_{2g} orbital degeneracy					
$n\mathrm{d}^1$	$n\mathrm{d}^2$	$n\mathrm{d}^4$ LS	$n\mathrm{d}^5$ LS	$n\mathrm{d}^6$ HS	$n\mathrm{d}^7$ HS
$MgTi_2O_4$	MgV_2O_4	–	$CuIr_2O_4$[a]	Fe_2O_3[a], $ZnCo_2O_4$[b]	$SiCo_2O_4$[b]
e_g orbital degeneracy					
$n\mathrm{d}^4$ HS	$n\mathrm{d}^7$ LS	$n\mathrm{d}^9$			
$ZnMn_2O_4$	–	–			

[a] Mixed with another valence state on the B site.
[b] The spin state assignment is uncertain.

and Mn(5)). Mn(1) (multiplicity 16) forms isolated sites, with a local distortion suggesting $d_{3z^2-r^2}$ orbital occupancy (the Mn(1)–O distances are 2.13 Å along the *c* axis and 1.96/1.88 Å in the plane). Mn(2) (multiplicity 32) forms isolated tetrahedra of four sites, with $d_{3x^2-r^2}$ orbital occupancy (the Mn(2)–O distances are 2.08/2.12 Å along the *a* axis, 1.96/1.88 Å along the *b* axis and 1.90/2.03 Å along the *c* axis). Mn(3) (multiplicity 32) forms continuous spirals running along the *c* axis, with $d_{3y^2-r^2}$ orbital occupancy (the Mn(3)–O distances are 2.16/2.22 Å along the *b* axis, 1.94/1.95 Å along the *a* axis and 1.90/1.95 Å along the *c* axis). Mn(4) and Mn(5), both with multiplicity 32, each forms an isolated dimer, which combines with the other to form isolated eight-member clusters. All Mn-O distances for these species are less than 2 Å, indicating a predominant 4+ character. It is noteworthy that there are more sites with 3+ character than those with 4+ (5/9 versus 4/9), indicating the failure of a naive ionic model of charge ordering (table 1).

The case of pure t_{2g} ions, which I will consider in detail in the remainder, is also very interesting. In these cases, B-site ions have partially filled t_{2g} and unfilled or half-filled e_g orbitals, leading to three-fold ground-state degeneracy. The contribution of the on-site JT energy is smaller than in the e_g case, since the orbitals do not point directly towards the ligands, and inter-ion energetic contributions can therefore become relevant. In principle, the following electronic configurations fulfil this condition: $n\mathrm{d}^1$, $n\mathrm{d}^2$, $n\mathrm{d}^4{}_{\mathrm{LS}}$, $n\mathrm{d}^5{}_{\mathrm{LS}}$, $n\mathrm{d}^6{}_{\mathrm{HS}}$ and $n\mathrm{d}^7{}_{\mathrm{HS}}$.[3] Up to now, only spinels containing Ti^{3+} ($3d^1$), V^{3+} ($3d^2$), Ir^{4+} ($5d^5$) and Fe^{2+} ($3d^6{}_{\mathrm{HS}}$) have been considered, but more systems may be waiting to be studied in the light of possible OO configurations.

In the presence of OO, electron hopping is only possible in certain directions at best, and this stabilizes non-metallic states. Conversely, most known metallic spinels have the undistorted $Fd\bar{3}m$ cubic structure. In t_{2g} transition-metal spinels, one would expect the metallic character to be controlled by the direct overlap of the t_{2g} orbitals, which, in turn, depends on the metal–metal

[3] HS and LS stand for high spin and low spin, respectively. In HS configurations, the Hund's rule coupling dominates over the crystal field splitting, and parallel-spin states (up to $n = 5$) will be filled before antiparallel states. In LS configurations, the crystal field splitting dominates over the Hund's rule coupling. In octahedral coordination, this means that the t_{2g} states will be filled first (up to $n = 6$).

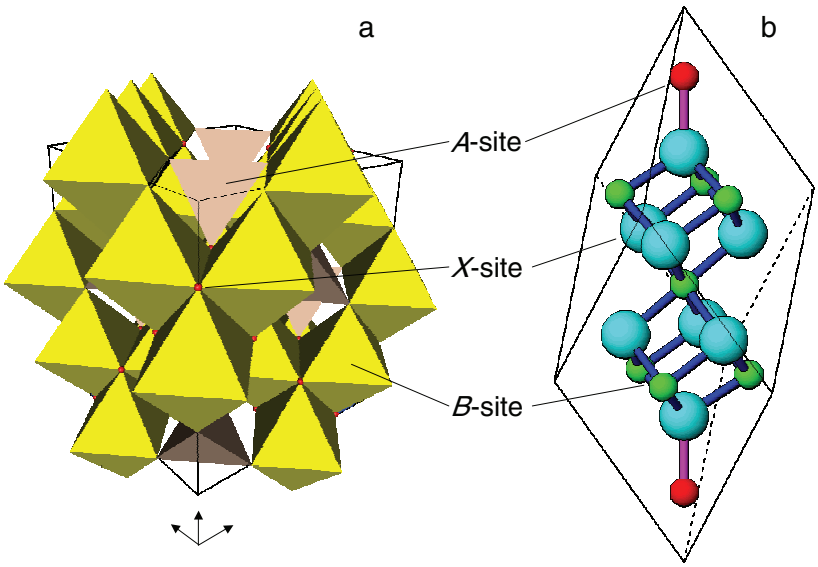

Figure 1. Two views of the undistorted spinel structure (general formula AB_2X_4). (a) The F-centred cubic unit cell ($Z = 8$). The A and B sites are at the centre of the tetrahedra and octahedra, respectively. The anion (X) site is at the corners of the polyhedra. (b) The primitive rhombohedral unit cell ($Z = 2$). It is noteworthy that the B-site ion is at the centre of a rhombohedrally distorted octahedron with D_{3d} ($\bar{3}$m) symmetry.

distance [21]. The relative size of the B cation and of the anion should play a key role, but few, if any, systematic studies of this effect exist [22].

3. Crystal-structure effects on the electronic structure

The first signature of possible OO in a variety of systems is a structural phase transition upon cooling. In spinels, the high-temperature phase is usually cubic, but a number of low-temperature structures have been observed. In cubic spinels (space group Fd$\bar{3}$m, no. 227 in the International Tables [23]), the transition metal's environment is not perfectly octahedral, since the B site has rhombohedral ($D_{3d} \equiv \bar{3}$m) point group symmetry (figure 1). In addition to the e_g/t_{2g} splitting arising from the roughly octahedral coordination around the B site, the rhombohedral crystal field further splits the d levels. Particularly, the low-lying t_{2g} triplet is split into a singlet (a_{1g}) and a doublet (e_g'). Unlike the case of the e_g/t_{2g} splitting, it is difficult to determine *a priori* which of these two orbitals has the lowest energy and what is the energy gap. In the extended spinel lattice, it is generally assumed that the a_{1g}/e_g' splitting is smaller than the width of the electronic bands, which originate mainly from direct overlap of the t_{2g} levels, since their lobes point directly towards an adjacent B site in the pyrochlore lattice.

The most common distortion of the spinel structure is by far the tetragonal distortion, whereby one of the cubic axes would become compressed or elongated with respect to the other two. If no additional symmetry breaking occurs, the tetragonal distortion alone decreases the symmetry from Fd$\bar{3}$m ($Z = 8$) to $I4_1/amd$ ($Z = 4$, see figure 2). This tetragonal distortion is

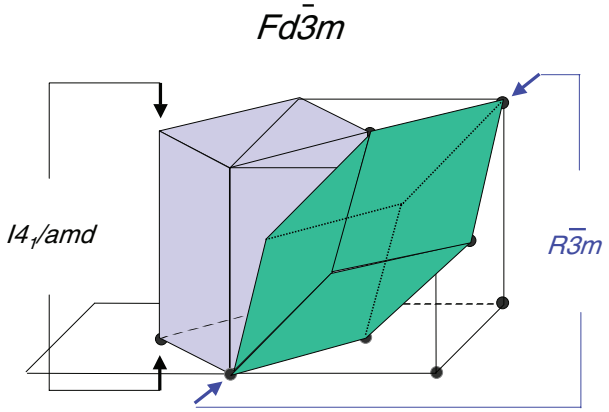

Figure 2. Geometrical relations between the undistorted F-centred Fd$\bar{3}$m cubic cell ($Z = 8$) and two possible distorted cells: the tetragonal I4$_1$/amd cell ($Z = 4$) results from a compression or extension of one of the [100] cubic axes. The rhombohedral R$\bar{3}$m cell ($Z = 2$) would result from a compression or extension along the cubic [1 1 1] diagonal. All three cells share the same primitive cell.

Table 2. Electronic configurations, lattice distortion and orbital character for OO spinels. The 'predicted' distortions and orbital characters are based on the on-site JT effect (see text). The 'observed' orbital character is from band structure calculations, on the basis of the observed crystallographic structure.

		$c/a\sqrt{2}$		Orbital character	
	Configuration	Predicted	Measured	Predicted	Observed
CdV_2O_4	$3d^2$	>1	0.9877	$d_{xz}{}^1d_{yz}{}^1$	$d_{xy}{}^1d_{xz}{}^1$ or $d_{xy}{}^1d_{yz}{}^{1a}$
ZnV_2O_4	$3d^2$	>1	0.9948	$d_{xz}{}^1d_{yz}{}^1$	$d_{xy}{}^1d_{xz}{}^1$ or $d_{xy}{}^1d_{yz}{}^{1a}$
$CuIr_2S_4$	$5d^5$ (+4 only)	>1	1.0333[b]	$d_{xy}{}^1d_{xz}{}^2d_{yz}{}^2$	$d_{xy}{}^1d_{xz}{}^2d_{yz}{}^2$
$MgTi_2O_4$	$3d^1$	<1	0.9963	$d_{xy}{}^1$	$d_{xz}{}^1$ or $d_{yz}{}^1$

[a] Presumed based on partial structural information.
[b] Pseudo-tetragonal.

thought to have a far more significant effect on the electronic structure than the local rhombohedral distortion of the octahedra. Upon c axis compression, the xz and yz orbitals, having a component along the c axis, will be raised in energy and broadened with respect to the xy orbitals, and the opposite will be true for a c-axis-stretched tetragonal structure, resulting, in both cases, in a splitting of the t_{2g} orbitals into a singlet and a doublet. If the JT effect was the dominant factor in driving the phase transition, one might expect the resulting state to have no orbital degeneracy. This would mean a tetragonal compression (i.e., $c/a\sqrt{2} < 1$) for nd^1, $nd^4{}_{LS}$ and $nd^6{}_{HS}$ and a tetragonal elongation (i.e., $c/a\sqrt{2} > 1$) for nd^2, $nd^5{}_{LS}$ and $nd^7{}_{HS}$. The experimental situation is in fact quite different (see table 2): there is a very poor correlation between the predicted and observed $c/a\sqrt{2}$ ratios. In the case of AZn_2O_4 (A = Zn, Mg, Cd), both the sign of the distortion [24]–[26] and the most probable orbital character of V in the distorted structure [27] are opposite

to the predictions. For $MgTi_2O_4$, the sign of the distortion is correct, but the orbital character (in this case confirmed by band structure calculations) is not. For $CuIr_2S_4$, both predictions are correct but, as we shall see, even in this case the JT distortion is not the dominant effect.

The tetragonal metric distortion is not the only possible one in spinels. For example, a pseudo-rhombohedral distortion is observed in both Fe_3O_4 [28, 29] and in AlV_2O_4 [30]. The authors give very different interpretations in the two systems: magneto-striction in the case of magnetite and charge ordering for the vanadate, but in both cases the origin of this distortion remains unclear.

4. Orbitally ordered configurations on a tetrahedron

Assuming that the electrons in the system are localized and that only *xy*, *xz* and *yz* orbitals are relevant (not their linear combinations), one might want to determine how many unique orbital configurations are possible on a single tetrahedron. The problem was considered by Di Matteo *et al* [31], who provide a description and a classification scheme for the case of $MgTi_2O_4$, where the number of occupied orbitals on each tetrahedron n_T is equal to 4. We will consider this problem in the general case as a function of n_T, whilst adopting the same classification scheme used by Di Matteo *et al* and under the assumption that there is no 'valence skipping', so that there are at most two adjacent valence states on the tetrahedron. These configurations can be classified according to the number of 'dimers', which are defined as pairs of sites, both having occupied orbitals with lobes along the bond that joins the sites. Therefore, if the 'dimer' bond between the two sites is along the *xy* direction, both sites will have occupied *xy* orbitals. We can further distinguish a 'symmetric' dimer bond (b_0), where the remaining orbitals are either absent or the same on both bonded sites, and an 'asymmetric' dimer bond (b_0', this notation is used for consistency with Di Matteo *et al*) in the remaining cases. In addition to the 'dimer' bond, three other types of bonds can be formed: either one site has one occupied orbital with lobes pointing along the bond, say *xy* in our example (b_1-type bond), or none of the sites has such an orbital. In the latter case, we can further distinguish a b_2-type bond if the sites have different orbital occupancy (e.g., one *xz* and one *yz* for an *xy*-oriented bond) and a b_3-type bond if the orbital occupancy is the same (say, both *xz* or both *yz*).

For $n_T = 1$, there is trivially a single possible configuration. The case $n_T = 2$ is also trivial: there are four possible configurations, depending on the type of bond (b_0, b_1, b_2 and b_3, since b_0' is not possible at less than double filling) between the two occupied sites. The case $n_T = 3$ is more interesting: since one of the sites is empty, this maps onto the problem of finding the unique orbital configurations on a triangle with edges *xy*, *yz* and *xz*. There are seven such configurations (see figure 3), which can, again, be classified according to the same scheme. B_1 and B_2 are one-dimer configurations, whilst C_1–C_5 are 0-dimer configurations. For $n_T = 4$ (single-valence case for nd^1, nd^4_{LS} and nd^6_{HS}), out of the 3^4 independent combinations of three orbitals on four sites, it can be shown that only six are topologically distinct for a tetrahedron (see figure 4): a single two-dimer configuration (A), three one-dimer configurations (B_1, B_2 and B_3) and two 0-dimer configurations (C_1 and C_2). For $n_T = 5$, there are 15 unique orbital configurations: a single two-dimer configuration, 11 one-dimer configurations and three 0-dimer configurations. For $n_T = 6$, there are 24 unique orbital configurations: a single three-dimer configuration, 11 two-dimer configurations, 11 one-dimer configurations and a single 0-dimer configuration. The remaining cases can be easily obtained from the previous ones by the symmetry between occupied and

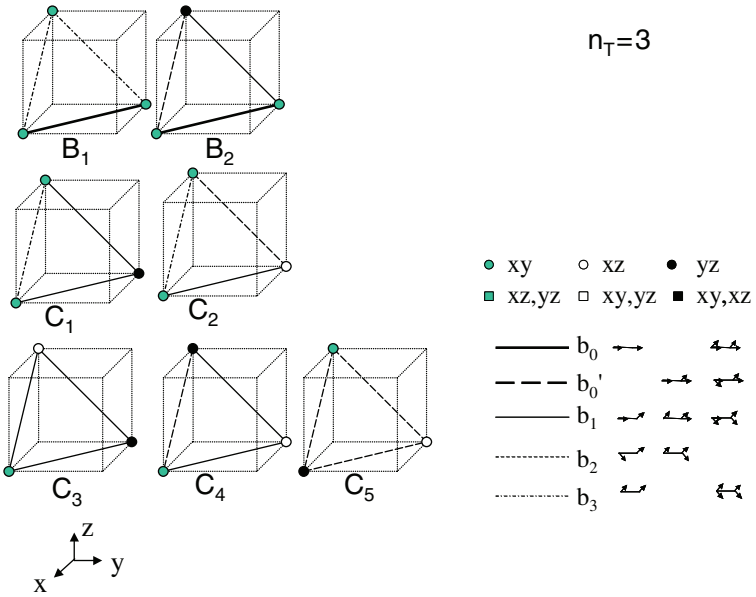

Figure 3. Orbitally ordered configurations on a tetrahedron accommodating three electrons ($n_T = 3$). ○ , □, singly and doubly occupied sites, respectively. Shading labels the unique occupied (or empty) orbital. Different styles of lines are used to indicate the different types of bonds (see the legend and text).

empty orbitals**.** The cases $n_T > 6$ can be obtained from $12-n_T < 6$ by replacing 'circles' with 'squares' and by making appropriate replacements to the bonds. I have reported in figure 5 only the case $n_T = 8$, which is the single-valence case for nd^2, $nd^5{}_{LS}$ and $nd^7{}_{HS}$ and is relevant for systems such as ZnV_2O_4.

5. Exchange interaction and chemical dimerization

The sign and strength of the magnetic exchange interactions resulting from different bonding configurations have also been considered by Di Matteo *et al* in the case of single orbital occupancy ($n_T \leqslant 4$) by using a Hamiltonian similar to the Kugel–Khomskii model [12]–[14] and values for the parameters that are considered by the authors as realistic. The strongest bond was found to be the 'dimer' bond b_0, which is antiferromagnetic (AFM), followed by the weaker FM b_1 bond. The other two bonds were found to be non-interacting in the approximation considered. The interaction between these tetrahedra in the extended pyrochlore lattice will be discussed in the section on $MgTi_2O_4$.

The formation of b_0-type bonds is known to lead in some cases to 'chemical' dimerization. This happens when stronger chemical bonds between pairs of metal sites are formed, associated with a doubly occupied molecular-like orbital and zero spin. It is well known, for example, that early transition metals in $3d^1$ electronic configuration (V^{4+}, Ti^{3+}) in edge- or face-sharing octahedral coordination display strong cation–cation interaction, which often leads to dimerization and spin pairing [21]. The classic example of this behaviour is VO_2(rutile structure, $V^{4+}3d^1$ $S = 1/2$), which undergoes a metal–insulator transition at 340 K, associated with a

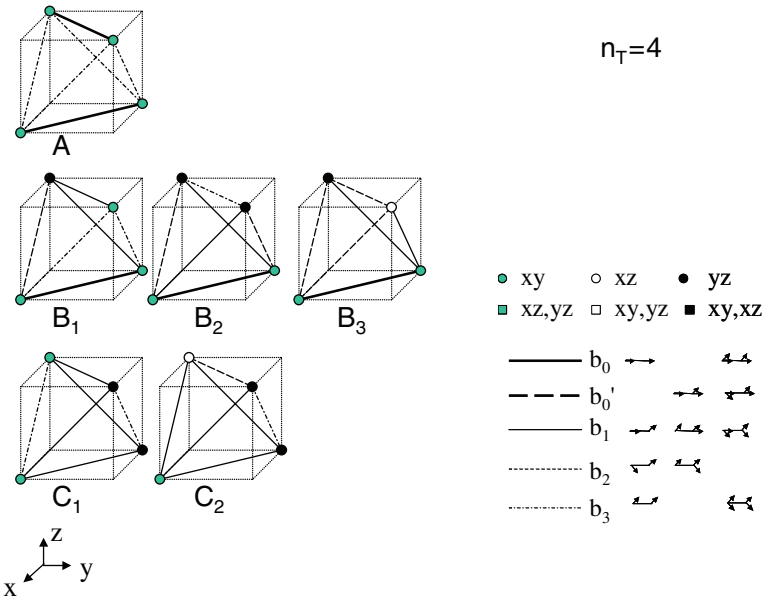

Figure 4. Orbitally ordered configurations on a tetrahedron accommodating four electrons ($n_T = 4$). Symbols are the same as in figure 3.

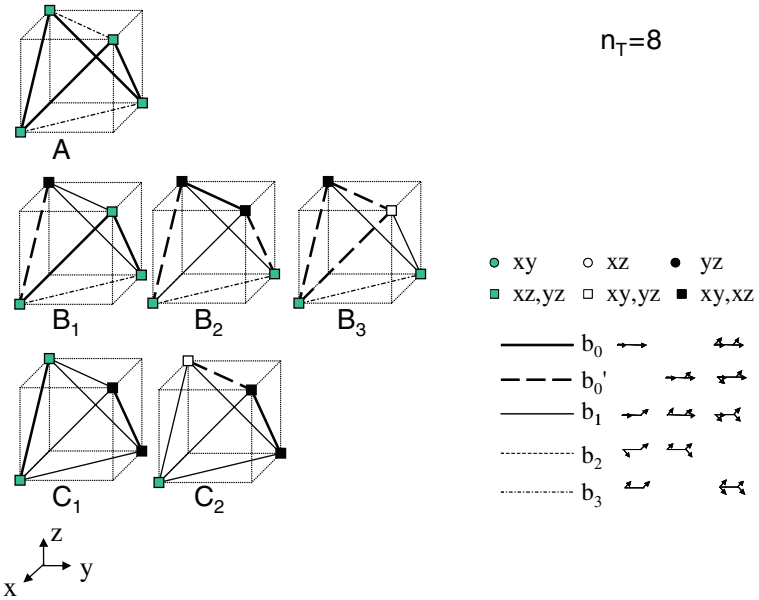

Figure 5. Orbitally ordered configurations on a tetrahedron accommodating eight electrons ($n_T = 8$). Symbols are the same as in figure 3.

structural transition from the high-temperature tetragonal structure to a monoclinic structure containing dimers with short V–V distances (2.65 Å) [32]. The V–V pairing is reflected in the magnetic susceptibility, which shows Curie–Weiss behaviour above T_c and a nearly constant van Vleck-like contribution below T_c, due to the formation of spin singlets associated with the V–V dimers. The rutile structure has a strong one-dimensional character, due to the presence of chains

of edge-sharing octahedra running along the tetragonal c axis. This leads to the splitting of the two-fold-degenerate t_{2g} band into a lower non-degenerate $d_{\|}$ band and an upper twofold-degenerate e_g^{π} band. Therefore, the transition in VO_2 can be described as a classic Peierls transition, associated with the splitting of the $d_{\|}$ band into bonding and anti-bonding branches, whilst the energy of the e_g^{π} band is further raised by the structural distortion [21], [33]–[35]. The structures of Ti_4O_7, V_4O_7 and other titanate and vanadate quasi-two-dimensional Magneli phases are also dimerized, but, being of mixed valence, they are charge-ordered at low temperatures. Ti_4O_7 is also thought to undergo a spin-dimerization and charge–localization transition at higher temperatures, towards a partially charge-disordered phase [36]. In analogy to the $3d^1$ configuration, low-spin cations in the nd^4_{LS} configuration (related to $3d^1$ by electron/hole symmetry) should also form dimers, although, to our knowledge, this was not established in the literature previous to the discovery of $CuIr_2S_4$ (see below). The case of nd^6_{HS} ions such as Fe^{2+} is clearly different, because the Pauli exclusion principle prevents the formation of singlets. It would still be possible for a b_0 bond to stabilize an AFM configuration, but this is strongly disfavoured if there is an underlying ferromagnetic ordering. This scenario will be further discussed with reference to the case of Fe_3O_4.

The case $n_T \geqslant 4$, where there is double orbital occupancy at least on some sites, has not, to our knowledge, been considered theoretically so far. The symmetry between $n_T = m$ and $n_T = 12 - m$ is useful for the purpose of generating all possible configurations, but here the analogy stops, because the bonding configurations are clearly different in the case of double orbital occupancy.

6. $MgTi_2O_4$

Although $MgTi_2O_4$ is one of the latest systems to be studied, I will consider it here before the others because of its relative simplicity. In this compound, Ti is in the 3+ oxidation state with $3d^1$ electronic configuration and $S = 1/2$, which makes it a strong candidate for single-valence dimerization. This compound is rather difficult to synthesize in pure form, due to the possibility of a (Ti, Mg) solid solution on the B site (all the compositions between $MgTi_2O_4$ and the Ti^{4+} inverse spinel $Mg(Ti, Mg)O_4$ can in fact be prepared). Before any good-quality sample became available, Tsunetsugu [37] examined the problem theoretically, as the limiting case of a collection of weakly interacting tetrahedra and under the assumption that the ground state is a spin liquid. In 2002, Isobe and Ueda [38] were finally able to synthesize a stoichiometric polycrystalline sample; its magnetic susceptibility presented a pronounced 'drop' upon cooling below $T_{MI} = 260$ K, strongly suggestive of the formation of magnetic singlets. At the same temperature, electrical resistivity measurements clearly showed a metal–insulator transition on cooling, coupled with a structural transition, which was detected using powder data collected with a laboratory diffractometer. The latter observation all but ruled out a spin liquid ground state, since geometrical frustration is most likely suppressed by the symmetry reduction. The low-temperature phase was found to be tetragonal, but there was no further analysis of the low-temperature symmetry in this work. We have re-examined this issue by using the more powerful synchrotron x-ray powder diffraction technique [39]. The metric distortion below T_M was found to be tetragonal, as reported by Isobe and Ueda. However, in addition to the splitting of the main cubic lines, we also detected additional super-structure peaks, which could all be indexed on a $a_c/\sqrt{2} \times a_c\sqrt{2} \times a_c$ primitive tetragonal unit cell, having half the volume of the cubic spinel cell. Unusually, the extinction conditions

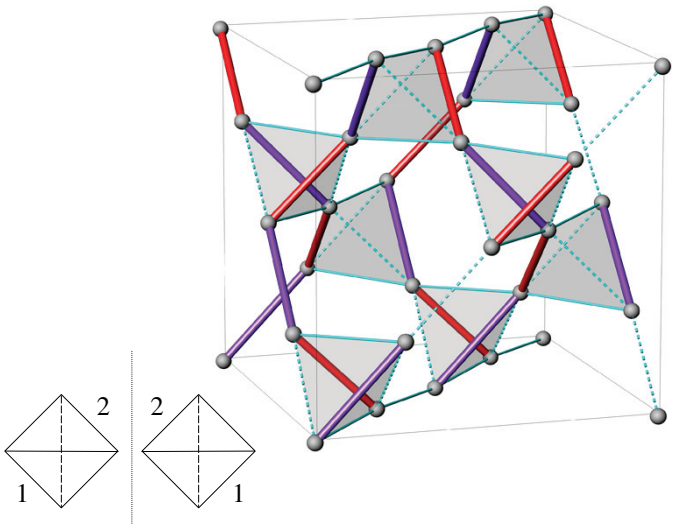

Figure 6. The dimerized structure of $MgTi_2O_4$ at low temperature (see [39]). The red and purple bonds represent the shortest (dimerized) and the longest bonds, respectively. The dashed and solid blue bonds mark the intermediate Ti–Ti distances. The inset shows how the distortion breaks the chiral symmetry of the individual tetrahedron. The point-group symmetry of a tetrahedron is T_d ($\bar{4}$3m) [23]. The tetragonal distortion decreases the symmetry to D_{2d} ($\bar{4}$2m). When bonds 1 and 2 become unequal, the symmetry is further reduced to the monoclinic point group C_2 (2). In this case, the tetrahedron cannot be transformed into its mirror image by rotation.

uniquely identify a pair of enantiomorphic, non-centrosymmetric space groups: $P4_12_12$ and $P4_32_12$, which are equivalent except for their chirality. The final structural refinement was performed by combining these data with high-resolution and medium-resolution neutron powder diffraction data, collected at the ISIS facility (UK). The structure contains only one Ti site, ruling out the possibility of charge disproportionation. However, the centre of symmetry at the Ti site is lost, so that Ti moves off the centre of the TiO_6 octahedron, and the six nearest-neighbour Ti–Ti distances become inequivalent. Two out of six Ti–Ti bonds (equal to 2.849(7) and 3.152(7) Å) differ substantially from the Ti–Ti distance found in the cubic $MgTi_2O_4$ (3.00362(1) Å). The shortest distance is comparable to the close-contact distance in Ti metal (2.896 Å at room temperature), suggesting the formation of a chemical dimer. From the point of view of crystallography, the observation of a chiral space group in an inorganic structure that does not inherently contain any chiral element is extremely unusual. Therefore, in describing the structure, we chose to focus on the issue of chirality. One of the many possibilities is to view this structure as a collection of 'helices' running along the *c* axis and as formed by an alternation of short and long bonds (figure 6). Perhaps better, one can recognize that each tetrahedron in the structure is inherently chiral once its symmetry is lowered to tetragonal and two opposite edges not orthogonal to the unique axis are selected (see inset and legend to figure 6). It is easy to see from figure 6 that all the tetrahedra have the same chirality, i.e., they can all be transformed into each other by rotations and translations. The structure is then uniquely

described by the single-valence condition, so that no Ti site can form more than one non-collinear dimer. Another way of describing the structure emerges from the observation that chains running in the [0 1 1], [0 1 $\bar{1}$], [1 0 1] and [1 0 $\bar{1}$] cubic directions are 'tetramerized' by an alternation of ... short–medium–long–medium ... bonds. As we will see, these descriptions are an important step in constructing OO models for this compound.

By analogy with VO_2 and the titanate Magneli phases, it is natural to speculate that the short bond in $MgTi_2O_4$ are associated with a spin singlet in a molecular-like orbital configuration. This was further confirmed by band structure calculations, as we have described in [39]. Electronic exchange and correlation were approximated using hybrid exchange density functional theory, by employing the B3LYP functional as implemented in the CRYSTAL code. These calculations confirmed that only *xz* and *yz* orbitals are occupied in the tetragonal structure while the $3d_{xy}$ states are pushed to higher energy. These results are readily interpreted on the basis of the observed crystal structure, by noting that the short Ti–Ti bonds have the same orientation as the occupied t_{2g} orbitals, alternating between the $3d_{yz}$ ($[0\,1\,1]_c$, $[0\,1\,1]_c$, $[0\,1\,\bar{1}]_c$) and $3d_{xz}$ ($[1\,0\,\bar{1}]_c$ and $[1\,0\,1]_c$) directions on different sites. This is consistent with orbital ordering, and with the short bonds becoming the location of zero-spin Hund–Mulliken (molecular-orbital-like) singlets.

The important issue is to understand why this particular OO configuration is favoured over all other possibilities. Di Matteo *et al* [31] consider this problem by calculating the energy of a collection of tetrahedra with different bonding configurations, as explained above. It may appear that the double-dimer 'A-type' configuration should be favoured by the AFM interaction. However, in this case, the dimers are not isolated, and the problem maps into a set of one-dimensional decoupled Heisenberg chains. It is shown that such a system has a higher energy per site than a collection of isolated 'B-type' tetrahedra. The degeneracy between different mixtures of B_1, B_2 and B_3 configurations is resolved in favour of a pure 'B_2-type' chiral arrangement by taking into account the lattice strain.

Another approach, proposed by Khomskii and Mizokawa [40], considers this system as being close to an itinerant state, and explains the distortion as originating from an orbitally driven Peierls transition. This provides a unified picture for both $MgTi_2O_4$ and $CuIr_2S_4$, and will be considered separately.

7. $CuIr_2S_4$

It has been known since the early 1990s that the $CuIr_2S_4$ thiospinel displays a metal–insulator (MI) transition at 230 K with an abrupt decrease of the electrical conductivity on cooling by more than two orders of magnitude [41]–[45]. The MI transition is also accompanied by the loss of localized magnetic moments. An important issue in interpreting the transition is the valence state of Ir, since both Cu and, in principle, S could have different valence states. The mixed-valence nature of the Ir ions (50% Ir^{3+} and 50% Ir^{4+}), together with a Cu valence of +1, have been established using spectroscopic methods [42]–[46]. Although none of these studies evidenced CO directly, CO became a natural hypothesis to explain the loss of conductivity. It has been speculated that spin dimerization between the magnetic Ir^{4+} ions might be a possible explanation for the loss of magnetic moment [41]–[43]. Hence, simultaneous charge ordering and spin dimerization has become an interesting possibility. Furubayashi *et al* [41] showed that the MI transition is associated with a sharp first-order structural transition, lowering the crystal symmetry from the cubic (space group $Fd\bar{3}m$) high-temperature phase. Furubayashi *et al*

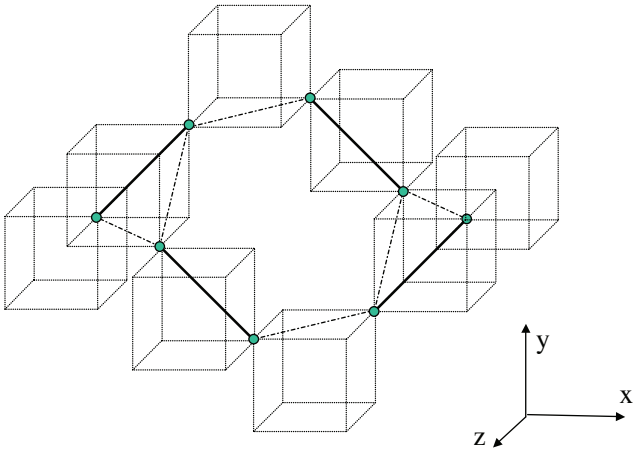

Figure 7. Construction of an 'octamer' from single-tetrahedron dimerized configurations. Only *xy* orbitals are employed. Tetrahedra with $n_T = 2$ have the simple dimerized configuration, whereas tetrahedra with $n_T = 3$ have the B_1 configuration in figure 3. Filled and empty sites are occupied by Ir^{4+} and Ir^{3+}, respectively.

proposed the tetragonal space group $I4_1/amd$ for the low-temperature structure, but also remarked the presence of unindexed Bragg peaks. The main metric distortion is a tetragonal elongation ($c > a\sqrt{2}$), although Ishibashi *et al* subsequently reported a triclinic symmetry [47]. We have solved the complete low-temperature structure of $CuIr_2S_4$ by using a combination of electron diffraction, high-resolution synchrotron x-ray powder diffraction, high- and medium-resolution neutron powder diffraction [48]. In agreement with Ishibashi *et al* [47], the crystal symmetry is triclinic ($P\bar{1}$) with lattice parameters $a = 11.95032(10)$ Å, $b = 6.98016(8)$ Å, $c = 11.92776(9)$ Å, $\alpha = 91.0550(7)^\circ$, $\beta = 108.4672(6)^\circ$ and $\gamma = 91.0320(7)^\circ$. A close examination of the refined structure reveals a remarkable complexity. There are eight independent Ir atoms in the triclinic structure. Of these, four form very short metal–metal bonds (~3.0 Å) with each other across shared octahedral faces, all the other Ir–Ir distances being between 3.43 and 3.66 Å. It is natural to assume that the dimerized Ir atoms have a valence of +4, forming singlet spin states, thus explaining the disappearance of the local magnetic moments. The two types of Ir, dimerized (Ir^{4+}) and non-dimerized (Ir^{3+}) are arranged in isovalent 'octamers' (groups of eight octahedra, related in pairs by the centre of symmetry), yielding a very unusual CO pattern. It is noteworthy that all the short bonds are oriented in the pseudo-tetragonal *ab* plane, which explains the tetragonal elongation. Furthermore, by analogy with the previous case, the unpaired electrons would occupy the d_{xy} orbitals, which are directed along the dimer bonds. If we examine the charge-ordering pattern, we find that not all the corner-sharing tetrahedra of the B site network satisfy the so-called Anderson condition [5], whereby each tetrahedron should be charge-balanced. In fact, each tetrahedron can contain one, two or three Ir^{4+} ions. Figure 7 illustrates how all the single-orbital configurations for $n_T = 1$, 2 and 3 are employed to construct the octamers (see also figure 3). Tetrahedra with $n_T = 2$ have either the b_0 or the b_3 configuration, whereas for $n_T = 3$ the only possible one-orbital configuration is A_1. Once again, each Ir^{4+} ion is involved in a single dimer bond. Whether the same could be accomplished with a collection of Anderson tetrahedra of b_0 and b_3 types is a non-trivial problem that needs further investigation. Interestingly, it has been

shown that disordered dimer arrangements can exist, at least as metastable phases. Ishibashi *et al* [49] have shown that it is possible to induce a transition from triclinic to tetragonal by shining x-rays at low temperatures on $CuIr_2S_4$ polycrystalline samples. This most likely comes about because the octamer pattern is destroyed, whilst Ir^{4+}–Ir^{4+} dimers persist with the same orientation but without long-range ordering.

The proposed model of charge and orbital ordering for the insulating $CuIr_2S_4$ was later found to be broadly consistent with the changes of the x-ray absorption spectra [50] and of the optical spectra [51] through the metal–insulator transition. From the latter data, one can also infer the size of the energy gap in the insulating phase ($\sim$0.15 eV). Band structure calculations using the LDA-DFT approach [52] give results compatible with these observations, but do not seem to support the naive model of charge ordering that we have proposed. One possibility put forth by the authors is that screening of the holes may occur to conceal the charge segregation at the scale of the atomic sphere by deforming the valence states. This is reminiscent of a recent interpretation of LDA + U calculations for Fe_3O_4 (see below) [53].

8. Charge and orbital ordering close to an itinerant state

Both charge and orbital ordering have been in the past the subject of much controversy. The main criticism levelled at these concepts is that the fully localized picture that is often employed to describe CO and OO patterns is very far from reality. The clearest manifestation of this is the fact that, no matter what technique is employed to determine the valences, one never observes integral values. In particular, there has been much discussion about the inability to observe charge disproportionation using XANES in a variety of systems [8]. In the manganites, CO and OO are observed by resonant scattering (see for example [54]), although the CO scenario of this recent work represents a significant departure from the 'traditional' view, as explained in section 1. CO is usually inferred from diffraction data, but bond valence sum calculations always return fractional valences [8]. Leonov *et al* [53] examine in detail the case of magnetite (see below), and suggest that some of the inconsistencies could be explained by the fact that the charge associated with the 'active' orbitals is effectively screened by the rearrangement of the other electrons. This would imply that the 'isotropic' CO (obtained by counting all electrons inside the atomic spheres) is always smaller than the one inferred from the OO pattern. Nevertheless, it seems clear that the localized picture fails in many cases, and it may be more appropriate to consider the phase transitions starting from the de-localized limit. This 'CO/OO from band picture' scenario bears much similarity to the Peierls transitions [55] where charge disproportionation is small and charge density waves originate from instabilities of the Fermi surface due to electron–phonon coupling. Since Peierls physics is critically dependent on the one-dimensional nature of the problem, it is natural to look for one-dimensional features in the electronic structures of these three-dimensional compounds to validate this picture. Indeed, it is known that electronic bands originating from direct overlap of t_{2g} orbitals in spinels have a strongly 1-D character. Khomskii and Mizokawa [40] exploit this feature to describe CO and OO in $CuIr_2S_4$ and $MgTi_2O_4$. A common feature of these two systems is that, once the structural distortion is taken into account, the electronic bands originating from the low-lying orbitals are quarter-filled by holes or electrons, respectively. To obtain this, it is crucial to assume a certain tetragonal distortion as given, and to take into account both the shift of the electronic levels and the change in bandwidth arising from the distortions. For $CuIr_2S_4$, the *xy* band, which can accommodate two electrons per site, becomes

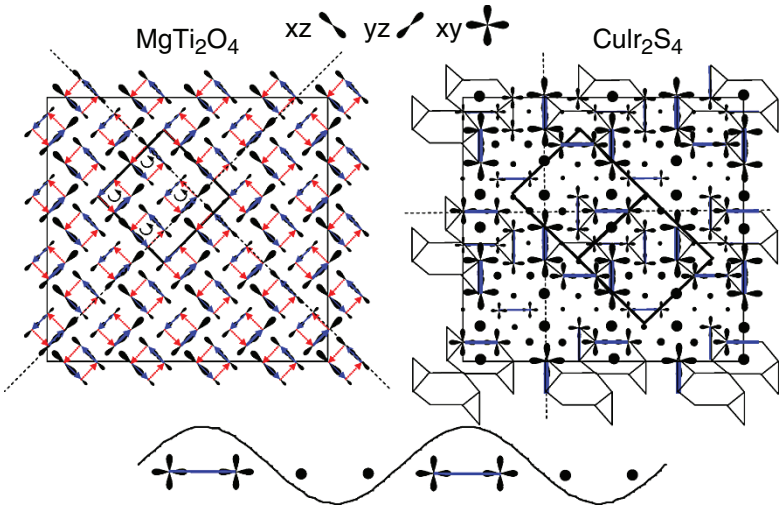

Figure 8. Orbital ordering in $MgTi_2O_4$ and $CuIr_2S_4$ in the tetramerization scheme proposed by Khomskii and Mizokawa [40]. The graphical representation is similar to the one used in [64], with a view down the [0 0 1] direction, but with the cubic axes at a 45° angle (the projection of the cubic unit cell edges is shown with thick lines). Smaller symbols represent atoms that are farther away from the plane of view. The tetramerization directions, where each orbital forms a bond-centred charge-density wave (shown below), are represented by dashed lines. For $MgTi_2O_4$, blue and red arrows represent short and long bonds, respectively, and the circular arrows indicated the chirality of the helices. For $CuIr_2S_4$, the 'octamers' are outlined.

broader and is shifted upwards, so it becomes occupied by 1.5 electrons per site (quarter-filling by holes), while the *xz* and *yz* bands are full. Likewise, in $MgTi_2O_4$, the *xz* and *yz* bands, which can accommodate four electrons per site, become broader and are occupied by one electron per site (quarter-filling by electrons). In both cases, the one-dimensional nature of the band would lead to an instability with wave vector $Q = \pi/2$ (i.e., quadrupling of the one-dimensional periodicity, or tetramerizaton), which can be described either as a bond-centred CDW or as a site-centred OO pattern (figure 8). Clearly, only $CuIr_2S_4$ can develop real CO and, as previously discussed, this may not be in the conventional sense.

9. Fe_3O_4

No review of OO on the pyrochlore lattice would be complete without mentioning the case of magnetite (Fe_3O_4), but a full review of over 60 years of research is beyond the scope of this work. The 3+ valence state for the tetrahedral Fe and, consequently, the mixed valence (2.5+) of the octahedral Fe, has now been established. However, the original charge-ordering hypothesis by Verwey [4] is still hotly debated, and Verwey's CO scheme is certainly not correct. Fe^{3+} is in the $3d^5{}_{HS}$ configuration and does not possess any orbital degree of freedom, but Fe^{2+} ($3d^6{}_{HS}$) does, so both CO and OO are possible in this system. The most recent structural model was

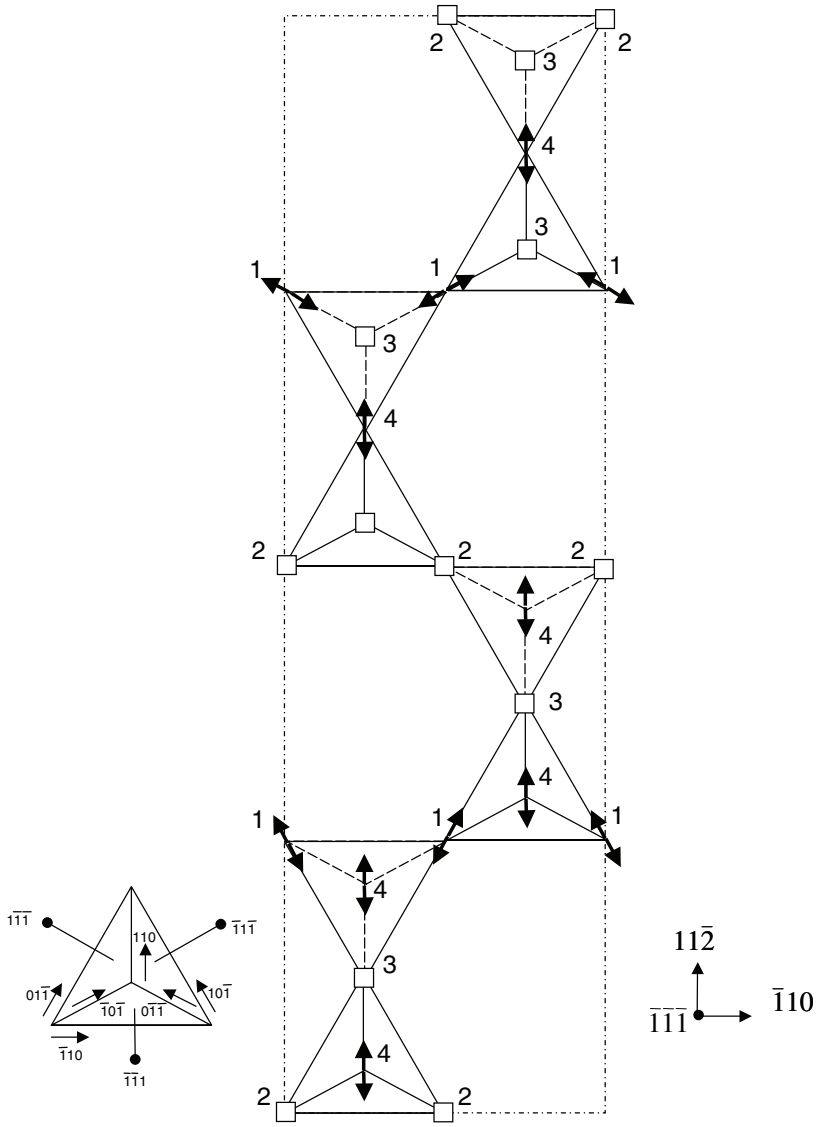

Figure 9. Charge and orbitally ordered pattern in Fe_3O_4, according to Wright *et al* [29] and Leonov *et al* [53]. The structure is projected onto the [111] planes to show the Kagomé lattice. Sites with arrows and squares have a 2+ and 3+ character, respectively. Each valence state forms isolated 'stripes', completely surrounded by the other valence state. The direction of the arrows indicates preferential orbital occupancy on the '2+' sites.

proposed by Iizumi *et al* [7] in 1982, based on single-crystal neutron diffraction data, but no CO pattern emerged naturally from this solution. Recently, Wright *et al* refined essentially the same model based on combined high-resolution neutron and x-ray diffraction data [29, 56]. This time, by employing the bond valence sum method [57], it was possible to distinguish a weak charge modulation. Interestingly, this modulation breaks up the structure in one-dimensional 'stripes' with 2+ and 3+ character (figure 9). This interpretation has been the subject of much controversy [8]. Very recently, Leonov *et al* [53] employed this structural model as a basis for an LDA + U

calculation of the electronic structure. The weak CO fluctuation was reproduced in the electronic structure, which amounts to a validation of the BVS procedure. However, Leonov *et al* obtained a much less trivial result: the t_{2g} occupancy is strongly modulated between the formally '3+' and '2+' sites, yielding a distinct OO pattern. This was found to contain b_1 bonds and to lack any b_0 bond, an arrangement that is favoured by the underlying FM ordering of the spins. No direct experimental confirmation of this pattern is so far available. In fact, very recent x-ray resonant scattering results [58, 59] seem to rule out even the weak charge fluctuation implied by the works of Wright *et al* [29, 56] and Leonov *et al* [53]. The interpretation of these results is still open to debate. Nevertheless, in my opinion the results on Fe_3O_4 from different techniques are converging towards a modified picture of electronic ordering on different sites, similar to the aforementioned case of the manganites, with or without a charge density modulation.

10. AV_2O_4 (A = Mg, Zn, Cd)

In these materials, vanadium is in the single-valence 3+ state, with electronic configuration $3d^2$, as described in figure 5 ($n_T = 8$). All three compounds undergo two transitions in the magnetic susceptibility: for Cd, $T_{c1} = 97$ K, $T_{c2} = 35$ K; for Mg, $T_{c1} = 65$ K, $T_{c2} = 45$ K; for Zn, $T_{c1} = 52$ K and $T_{c2} = 44$ K [26]. It has long been known that these compounds are antiferromagnetic at low temperatures [60], and the low-temperature transition is usually attributed to the onset of magnetic order. In addition, all these systems undergo a cubic-to-tetragonal phase transition (with tetragonal compression, i.e., $c/a\sqrt{2} < 1$) on cooling [24]–[26]. The proposed space group for the low-temperature phase is $I4_1/amd$, which is the highest-symmetry tetragonal space group for the spinel structure, and does not give rise to new Bragg peaks in a diffraction experiment. The magnetic structure, first proposed by Niziol [60] and recently revisited by Reehius *et al* [61], entails a violation of the body-centring translation, as implied by the observation of the (1 0 0) and (1 1 1) magnetic Bragg peaks. The magnetic propagation vector is therefore $q = [0, 0, 1]$. The two magnetic modes proposed by Reehius *et al* are degenerate, and are generated by the Γ_2 representation in the Kovalev conventions [62] (the propagation vector group G_k is the same for the cubic and tetragonal structures). The moments are oriented along the tetragonal *c*-axis, and are less than half of the expected magnitude (0.65 instead of 2 μ_B). The structure is easy to visualize if one considers the ...V–V–V... 'chains' running along the [1 1 0]/[$\bar{1}$ 1 0] (or *xy*), [1 0 1]/[$\bar{1}$ 0 1] (*xz*) and [0 1 1]/[0$\bar{1}$1] (*yz*) directions of the original cubic structure. Chains in the *xy* directions order in the sequence ...+−+−+−... while those in the *xz* and *yz* directions order with the spin sequence ...++−−++−−.... Tsunetsugu and Motome [27] considered the problem by employing a Kugel–Khomskii Hamiltonian, similar to the approach of Di Matteo *et al* [31] for the case of $MgTi_2O_4$. First, the ground states for the orbital degrees of freedom are found for individual tetrahedra and in the hypothesis that the b_1-type bonds (antiferro-orbital configurations) are favoured. Then, the remaining orbital degeneracy (configurations B_1, B_2 and B_3 in figure 5 is lifted by the structural distortion, and configuration B_2 is stabilized. At this point, an orbital structure resulting from the assemblage of type B_2 tetrahedra is obtained uniquely: in this scheme, *xy* orbitals would be occupied on all sites, while *xz* and *yz* orbitals would be alternately occupied on different sites. Finally, this structure is examined for the most favourable spin ordering, which is found to correspond to the experimental structure. The scenario proposed by Tsunetsugu and Motome [27] is corroborated by recent inelastic neutron scattering experiments [63], showing that the spin excitation spectra become one-dimensional in character

below the structural transition, consistent with the formation of antiferromagnetic chains in the *xy* directions. Nevertheless, much doubt remains regarding the orbital structure proposed by Tsunetsugu and Motome [27]. The main issue is the symmetry of the crystal structure, which, in this scenario, should be $I4_1/a$, i.e., lower than the observed one. This issue is addressed by Tchernyshyov [64]; his alternative model, which takes into account the relativistic spin–orbit interaction, has $I4_1/amd$ crystallographic symmetry, and is able to account for the observed magnetic structure. Clearly, further insight may be provided by future experiments, which may reveal a previously unobserved symmetry lowering.

11. Conclusions

The study of orbital ordering in geometrically frustrated lattices has emerged quite rapidly in the last few years, and has already provided significant insight into apparently complex problems, by a unique combination of advanced experimental techniques and theoretical and computational modelling. By merging knowledge from a number of related fields in solid-state physics, such as that of metal–insulator transitions, Peierls and spin-Peierls transitions and geometrical frustration, new light is being shed onto old unsolved problems. For the first time in 60 years, the solution to the magnetite conundrum appears to be within reach. Nevertheless, many new systems will almost certainly emerge to challenge experimentalists and theoreticians alike, both in the spinel and in other crystal types. Among the latter, the pyrochlore $Tl_2Ru_2O_7$ is an interesting candidate for orbital ordering [65]. Although its phenomenology is very reminiscent of $MgTi_2O_4$, the connectivity of the Ru–O network is quite different, being corner-shared instead of edge-shared and displaying a much larger on-site trigonal distortion. One expects that research on this and other related systems will remain topical for many years to come.

Acknowledgments

I acknowledge the invaluable insights provided to me by Daniel Khomskii, Sergio Di Matteo and Martin Long in a series of discussions on the topics discussed in this paper. I also thank Laurent Chapon for extensively reviewing the manuscript.

References

[1] Ramirez A P 1994 *Ann. Rev. Mater. Sci.* **24** 453
[2] Pauling L 1935 *J. Am. Chem. Soc.* **57** 2680
[3] Bernal D and Fowler R H 1933 *J. Chem. Phys.* **1** 515
[4] Verwey E J W 1939 *Nature (London)* **144** 327
[5] Anderson P W 1956 *Phys. Rev.* **102** 1008
[6] Bramwell S T and Gingras M J P 2001 *Science* **294** 1495
[7] Iizumi M, Koetzle T F, Shirane G, Chikazumi S, Matsui M and Todo S 1982 *Acta Crystallogr. B.* **38** 2121
[8] Garcia J and Subias G 2004 *J. Phys.: Condens. Matter* **16** R145
[9] Khomskii D I and Mostovoy M V 2003 *J. Phys. A: Math. Gen.* **36** 9197
[10] Jahn H A and Teller E 1937 *Proc. R. Soc.* A **161** 220
[11] Goodenough J B 1955 *Phys. Rev.* **100** 564
[12] Kugel K I and Khomskii D I 1973 *Sov. Phys.—JETP* **37** 725
[13] Kugel K I and Khomskii D I 1975 *Sov. Phys.—Solid State* **17** 285

[14] Kugel K I and Khomskii D I 1982 *Sov. Phys.—Usp.* **25** 231
[15] Khaliullin G and Okamoto S 2003 *Phys. Rev.* B **68** 205109
[16] Paolasini L *et al* 1999 *Phys. Rev. Lett.* **82** 4719
[17] Di Matteo S, Perkins N B and Natoli C R 2002 *Phys. Rev.* B **65** 054413
[18] Nogues M and Poix P 1962 *J. Phys. Chem. Solids* **23** 711
[19] Nogues M and Poix P 1972 *Ann. Chim.* **1972** 301
[20] Rodriguez-Carvajal J, Rousse G, Masquelier C and Hervieu M 1998 *Phys. Rev. Lett.* **81** 4660
[21] Goodenough J B 1960 *Phys. Rev.* **117** 1442
[22] Shirane G and Cox D E 1964 *J. Appl. Phys.* **35** 954
[23] Hahn T 2002 *International tables for crystallography* vol A (Dodrecht: Kluwer Academic)
[24] Ueda Y, Fujiwara N and Yasuoka H 1997 *J. Phys. Soc. Japan* **66** 778
[25] Mamiya H and Onoda M 1995 *Solid State Commun.* **95** 217
[26] Nishiguchi N and Onoda M 2002 *J. Phys.: Condens. Matter* **14** L551
[27] Tsunetsugu H and Motome Y 2003 *Phys. Rev.* B **68** 060405
[28] Wright J P, Bell A M T and Attfield J P 2000 *Solid State Sci.* **2** 747
[29] Wright J P, Attfield J P and Radaelli P G 2002 *Phys. Rev.* B **66** 214422
[30] Matsuno K, Katsufuji T, Mori S, Moritomo Y, Machida A, Nishibori E, Takata M, Sakata M, Yamamoto N and Takagi H 2001 *J. Phys. Soc. Japan* **70** 1456
[31] Di Matteo S, Jackeli G, Lacroix C and Perkins N B 2004 *Phys. Rev. Lett.* **93** 077208
[32] Westman S 1961 *Acta Chem. Scand.* **15** 217
[33] Gupta M, Freeman A J and Ellis D E 1977 *Phys. Rev.* B **16** 3338
[34] Wentzcovitch R M, Schultz W W and Allen P B 1994 *Phys. Rev. Lett.* **72** 3389
[35] Eyert V 2002 *Ann. Physik* **11** 650
[36] Marezio M, McWhan D B, Dernier P D and Remeika J P 1972 *Phys. Rev. Lett.* **28** 1390
[37] Tsunetsugu H 2001 *J. Phys. Soc. Japan* **70** 640
[38] Isobe M and Ueda Y 2002 *J. Phys. Soc. Japan* **71** 1848
[39] Schmidt M, Ratcliff W, Radaelli P G, Refson K, Harrison N M and Cheong S W 2004 *Phys. Rev. Lett.* **92** 056402
[40] Khomskii D I and Mizokawa T 2004 *Preprint* cond-mat/0407458
[41] Furubayashi T, Matsumoto T, Hagino T and Nagata S 1994 *J. Phys. Soc. Japan* **63** 3333
[42] Matsuno J, Mizokawa T, Fujimori A, Zatsepin D A, Galakhov V R, Kurmaev E Z, Kato Y and Nagata S 1997 *Phys. Rev.* B **55** R15979
[43] Nagata S, Matsumoto N, Kato Y, Furubayashi T, Matsumoto T, Sanchez J P and Vulliet P 1998 *Phys. Rev.* B **58** 6844
[44] Matsumoto N, Endoh R, Nagata S, Furubayashi T and Matsumoto T 1999 *Phys. Rev.* B **60** 5258
[45] Burkov A T, Nakama T, Hedo M, Shintani K, Yagasaki K, Matsumoto N and Nagata S 2000 *Phys. Rev.* B **61** 10049
[46] Kumagai K, Kakuyanagi K, Endoh R and Nagata S 2000 *Physica* C **341** 741
[47] Ishibashi H, Sakai T and Nakahigashi K 2001 *J. Magn. Magn. Mater.* **226–230** 233
[48] Radaelli P G, Horibe Y, Gutmann M J, Ishibashi H, Chen C H, Ibberson R M, Koyama Y, Hor Y S, Kiryukhin V and Cheong S W 2002 *Nature* **416** 155
[49] Ishibashi H, Koo T Y, Hor Y S, Borissov A, Radaelli P G, Horibe Y, Cheong S W and Kiryukhin V 2002 *Phys. Rev.* B **66** 144424
[50] Croft M, Caliebe W, Woo H, Tyson T A, Sills D, Hor Y S, Cheong S W, Kiryukhin V and Oh S J 2003 *Phys. Rev.* B **67** 201102
[51] Wang N L, Cao G H, Zheng P, Li G, Fang Z, Xiang T, Kitazawa H and Matsumoto T 2004 *Phys. Rev.* B **69** 153104
[52] Sasaki T, Arai M, Furubayashi T and Matsumoto T 2004 *J. Phys. Soc. Japan* **73** 1875
[53] Leonov I, Yaresko A N, Antonov V N, Korotin M A and Anisimov V I 2004 *Phys. Rev. Lett.* **93** 146404
[54] Grenier S *et al* 2004 *Phys. Rev.* B **69** 134419

[55] Peierls R E 1955 *Quantum Theory of Solids* (Oxford: Oxford University Press)
[56] Wright J P, Attfield J P and Radaelli P G 2001 *Phys. Rev. Lett.* **87** 266401
[57] Brown I D 1989 *J. Solid State Chem.* **82** 122
[58] Subias G, Garcia J, Blasco J, Proietti M G, Renevier H and Sanchez M C 2004 *Phys. Rev. Lett.* **93** 156408
[59] Subias G, Garcia J, Proietti M G, Blasco J, Renevier H, Hodeau J L and Sanchez M C 2004 *Phys. Rev.* B **70** 155105
[60] Niziol S 1973 *Phys. Status Solidi* A **18** K11
[61] Reehuis M, Krimmel A, Buttgen N, Loidl A and Prokofiev A 2003 *Eur. Phys. J.* B **35** 311
[62] Kovalev O V 1965 *Irreducible Representations of the Space Groups* (London: Gordon and Breach)
[63] Lee S H *et al* 2004 *Phys. Rev. Lett.* **93** 156407
[64] Tchernyshyov O 2004 *Phys. Rev. Lett.* **93** 157206
[65] Takeda T, Kanno R, Kawamoto Y, Takano M, Izumi F, Sleight A W and Hewat A W 1999 *J. Mater. Chem.* **9** 215